JCTC Journal of Chemical Theory and Computation

Article

pubs.acs.org/JCTC

# Exploring the Limits of Density Functional Approximations for Interaction Energies of Molecular Precursors to Organic Electronics

Stephan N. Steinmann* and Clemence Corminboeuf*

Laboratory for Computational Molecular Design, Institut des Sciences et Ingénierie Chimiques, Ecole Polytechnique Fédérale de Lausanne, CH-1015 Lausanne, Switzerland

Supporting Information

**ABSTRACT:** Neutral and charged assemblies of $\pi$-conjugated molecules span the field of organic electronics. Electronic structure computations can provide valuable information regarding the nature of the intermolecular interactions within molecular precursors to organic electronics. Here, we introduce a database of neutral (Pi29n) and radical (Orel26rad) dimer complexes that represent binding energies between organic functional units. The new benchmarks are used to test approximate electronic structure methods. Achieving accurate interaction energies for neutral complexes (Pi29n) is straightforward, so long as dispersion interactions are properly taken into account. However, $\pi$-dimer radical cations (Orel26rad) are examples of highly challenging situations for density functional approximations. The role of dispersion corrections is crucial, yet simultaneously long-range corrected exchange schemes are necessary to provide the proper dimer dissociation behavior. Nevertheless, long-range corrected functionals seriously underestimate the binding energy of Orel26rad at equilibrium geometries. In fact, only $\omega$B97X-D, an empirical exchange-correlation functional fitted together with an empirical "classical" dispersion correction, leads to suitable results. Valuable alternatives are the more demanding MP2/6-31G*(0.25) level, as well as the most cost-effective combination involving a dispersion corrected long-range functional together with a smaller practical size basis set (e.g., LC-$\omega$PBEB95-dDsC/6-31G*). The Orel26rad test set should serve as an ideal benchmark for assessing the performance of improved schemes.

## INTRODUCTION

The rapidly growing field of organic electronics is dominated by $\pi$-conjugated molecules, which, because of their attractive properties, represent ideal functional units in molecular wires, organic solar cells, organic light-emitting diodes, and organic field-effect transistors.[1−3] Similarly, molecular switches, motors and artificial muscles typically rely on $\pi$-functional frameworks for converting an optical or electrochemical signal into a mechanical response.[4−8] Electronic structure computations provide routes to valuable information regarding the nature of the intermolecular interactions within molecular precursors to organic electronics, where neutral dimers model the resting state and charged radical $\pi$-dimers represent typical charge-carriers (i.e., the ultimate functional units).

Kohn−Sham density functional theory[9] (DFT) is the most popular electronic structure method for describing structures and properties of relatively large systems, including $\pi$-functional molecules and materials. Despite their ability to provide computationally efficient access to many ground state properties with reasonable accuracy, standard DFT approximations do not perform well in describing the interaction energies of $\pi$-conjugated molecules. The most obvious failures arise in assembled neutral monomers (e.g., dimers), where van der Waals interactions contribute substantially to the total binding energy. However, the most used semilocal (hybrid) functionals are intrinsically unable to accurately describe these nonlocal dispersion forces.[10−13] Fortunately, the neglected interactions can be conveniently accounted for by *a posteriori* atom pairwise dispersion corrections.[14−20] Our recently introduced density dependent dispersion correction, dDsC,[20−22] improves the performance of standard density functionals dramatically for describing both intermolecular interactions and reaction energies.[20,23] Hybrid functionals, when combined with dDsC, also succeed in describing the ground-state interaction energy of charge-transfer complexes, as illustrated by the prototypical tetrathiafulvalene-tetracyanoquinodimethane (TTF-TCNQ) complex.[24]

In this article, our primary focus is placed on the investigation of binding energies of $\pi$-dimer radical cations, such as $(\text{thiophene})_2^{\bullet+}$, which are formally mixed valence dimers. Standard density functionals fail to properly handle systems with fractional charges: at large intermolecular distances, the delocalization (or self-interaction) error artificially stabilizes one positive charge delocalized over two molecules in comparison to a situation with one positively charged and one neutral molecule.[25−28] Around equilibrium, the errors are smaller, but the description of mixed valence states remains subtle. Doubly charged $\pi$-dimers (e.g., tetracyanoethylene, $(\text{TCNE})_2^{2-}$)[29] present yet another issue, that is, the static correlation error.[30] In this case, the dissociation of singlet $(\text{TCNE})_2^{2-}$ is essentially not possible without breaking spin symmetry. Such dimers are difficult to describe even around equilibrium due to an important degree of multireference character.[31−33] In addition, doubly charged dimers tend to be unstable in the gas-phase due to Coulomb repulsion and are therefore excluded from this benchmark study.

Taken together, the failures of standard density functionals for dispersion interactions, mixed valence states, and multi-

**Received:** July 27, 2012
**Published:** October 3, 2012

reference character, the prospect for investigating $\pi$-functional molecules with standard DFT approximations appears rather discouraging. However, the size of the materials of practical interest precludes the application of generally robust, highly accurate ab initio methods to compute binding energies (e.g., CASPT2 or multireference coupled cluster). Herein, we present a benchmarking study to identify the best available modern functionals that are applicable to reproducing interaction energies of "real world" systems. Since the typical test sets representative of noncovalent interactions are dominated by biorelated model compounds, we introduce two benchmark sets of interaction energies: Orel26rad and Pi29n. Orel26rad features 26 radical cation model compounds for charge-carriers in organic electronics, while the under-representation of neutral sulfur containing heterocycles (e.g., thiophene[34]) and naphthalene complexes[35,36] in common test sets (e.g., S22[37]) prompted the introduction of an additional set of 29 binding energies of neutral intermolecular complexes (Pi29n). The new databases allow for a thorough assessment of the capabilities of density functionals to describe the interaction energies relevant for organic electronic precursors.

## METHODS AND COMPUTATIONAL DETAILS

**Construction of the Test Set.** All monomers are optimized at the B3LYP/6-31G* level[38−41] in Gaussian 09,[42] except for TTF-TCNQ, which is taken from our previously published equilibrium geometry.[24] The optimized geometries of the neutral and cationic monomers are used to construct the test sets without further relaxation: the radical dimer cations are built from the geometry of one neutral and one cationic monomer. Intermolecular distances and relative orientations were either taken from the literature (thiophene dimers,[34] naphthalene dimers,[35] and naphthalene···benzene complexes[36]) or obtained from scans (steps of 0.1 Å) at the counterpoise corrected df-MP2/6-31G*(0.25) level of theory. In general, the monomer centers are superimposed and only the intermolecular distance is optimized. Exceptions are the parallel thiophene···benzene (T-Bz_P), the (anti)-parallel thiophene···pyridine complexes (T-Py_P and T-Py_AP), and the second antiparallel thiophene dimer radical cation ($T_2$_AP2$^{\bullet+}$) for which the relative displacement was optimized as well (see Table 1 for the explanations of the abbreviations). For the T-shaped radical cations the stem and bar correspond to the neutral and radical cation monomer geometry, respectively.

**Table 1. Abbreviations for Monomers and Their Relative Orientation Used to Identify Dimers Included in the Two Test Sets Orel26rad and Pi29n**

| abbrev. | definition | abbrev. | definition |
|---|---|---|---|
| F | furan | S | slipped |
| T | thiophene | P | parallel |
| bz | benzene | AP | antiparallel |
| Py | pyridine | X | cross |
| Pyr | pyrrole | T | T-shape (heteroatom down) |
| bF | bifuran | T′ | T-shape (heteroatom up) |
| bT | bithiophene | | |
| TT | thienothiophene | •+ | radical cation |
| TTF | tetrathiafulvalene | | |
| TCNQ | tetracyanoquinodimethane | | |

**Benchmark Computations.** The highest computational level uniformly applicable for all dimers studied herein, is an estimated CCSD(T)/CBS interaction energy, which we denote by CCSD(T)*. The MP2 interaction energy is extrapolated to the CBS limit exploiting the efficiency of density-fitting (df)[43] and corrected by the $\delta$CCSD(T) term from a much smaller basis set

$$\Delta E(\mathrm{CCSD(T)^*}) = \Delta E(\mathrm{HF/AVQZ}) + \Delta E(\mathrm{df\text{-}MP2/CBS}) + \delta\mathrm{CCSD(T)/6\text{-}31G^*(0.25)}$$

The complete basis set extrapolation is carried out with aug-cc-pVTZ and aug-cc-pVQZ (AVTZ and AVQZ, respectively) according to the Helgaker scheme,[44] and the higher-order correlation correction $\delta$CCSD(T)/6-31G*(0.25) corresponds to the difference between MP2 and CCSD(T) in the 6-31G*(0.25) basis set, where (0.25) indicates the exponent of the set of d-orbitals added to the 6-31G basis set for all atoms except hydrogen.[45,46] All components are corrected for the basis set superposition error (BSSE) according to the Boys−Bernardi procedure.[47] Ab initio computations used the Molpro2010.1[48] defaults for auxiliary basis sets and technical parameters. For df-MP2/6-31G*(0.25), the auxiliary basis set of aug-cc-pVDZ has been applied.

The equation of motion for ionization potentials (EOM-IP) coupled cluster method is specifically designed to describe neutral and ionized species at a comparable level of accuracy. To validate the use of single reference CCSD(T)* as a benchmark level, the interaction energy of the benzene dimer cation was computed with CCSD(T), EOM-IP-CCSD,[49,50] and EOM-IP-CCSD(2,3)[51] in the small 6-31G*(0.25) basis set. The results at the three levels do not differ by more than about 1 kcal mol$^{-1}$, suggesting good accuracy of CCSD(T) for the radical cations. Note, that spin-contamination is largely avoided given that open-shell systems are treated in the RMP2[52] and ROHF-UCCSD(T)[53,54] framework. A breakdown of the single-reference treatment was observed for pyridine···pyridine$^{\bullet+}$ complex, which is described as unbound and has therefore been dropped from the test set.

**Symmetry Adapted Perturbation Theory.** Symmetry adapted perturbation theory (SAPT)[55] is an ab initio method that decomposes the interaction energy between molecules based on perturbation theory. At the SAPT0 level, there are six terms contributing to the interaction energy: classic electrostatics $E_{\mathrm{elst}}^{(10)}$ (electron−electron and nuclei−nuclei repulsion, counterbalanced by electron−nuclei attraction), exchange $E_{\mathrm{exch}}^{(10)}$ (arising from satisfying the Pauli-exclusion principle), induction $E_{\mathrm{ind}}^{(20)}$ (equivalent to polarization or charge-transfer in other terminologies), exchange−induction $E_{\mathrm{exch-ind}}^{(20)}$ (the correction for keeping the wave function antisymmetric), and finally dispersion $E_{\mathrm{disp}}^{(20)}$ and exchange−dispersion $E_{\mathrm{disp-exch}}^{(20)}$, accounting for the correlated motion of electrons between the two monomers.

$$E_{\mathrm{int}}^{\mathrm{SAPT0}} = E_{\mathrm{elst}}^{(10)} + E_{\mathrm{exch}}^{(10)} + E_{\mathrm{ind}}^{(20)} + E_{\mathrm{exch-ind}}^{(20)} + E_{\mathrm{disp}}^{(20)} + E_{\mathrm{disp-exch}}^{(20)} \quad (1)$$

For strongly interacting fragments, the $\delta^{\mathrm{HF}}$ term[56,57]

$$\delta^{\mathrm{HF}} = E^{\mathrm{HF}} - \left(E_{\mathrm{elst}}^{(10)} + E_{\mathrm{exch}}^{(10)} + E_{\mathrm{ind}}^{(20)} + E_{\mathrm{exch-ind}}^{(20)}\right) \quad (2)$$

which is the difference between the (counterpoise corrected) HF interaction energy and the electrostatics; exchange and

(exchange−)induction are often necessary to achieve agreement with supermolecular approaches. $E(\mathrm{SAPT0}) + \delta^{\mathrm{HF}}$ corresponds to Hartree−Fock plus the SAPT0 (exchange−)dispersion interaction and is denoted by HF + Disp herein.

$$E_{\mathrm{int}}^{\mathrm{HF+Disp}} = E^{\mathrm{HF}} + E_{\mathrm{disp}}^{(20)} + E_{\mathrm{disp-exch}}^{(20)} \tag{3}$$

Open-shell SAPT0[58] computations were performed in SAPT 2008.1, interfaced with Dalton 2.0,[59] using the 6-31G*(0.25) basis set.[45] Akin to MP2, SAPT0 is known to provide more accurate results in modest basis sets than at the complete basis set limit for neutral complexes of $\pi$-conjugated systems.[60,61] Since MP2/6-31G*(0.25) is accurate for the radical cations studied herein (vide infra), SAPT0 in the same, small basis set is expected to yield reasonable results as well. Note that we use SAPT0 with uncoupled response functions ("MP2-like"), as the coupled induction and dispersion energies do not benefit from the invoked error cancellation. For example, the dispersion energy is given by

$$E_{\mathrm{disp}}^{(20)} = -4 \sum_{ia,jb} \frac{|(i^{\mathrm{A}} a^{\mathrm{A}}|j^{\mathrm{B}} b^{B})|^2}{\varepsilon_a^{\mathrm{A}} - \varepsilon_i^{\mathrm{A}} + \varepsilon_b^{\mathrm{B}} - \varepsilon_j^{\mathrm{B}}} \tag{4}$$

where $i,j$ and $a,b$ are occupied and unoccupied orbitals, respectively, $(ia|jb)$ is the two-electron repulsion integral in chemist's notation, and $\varepsilon_i$ is the $i^{\mathrm{th}}$ orbital energy, while A and B labels the two monomers.

**Density Functionals Tested.** In addition to the standard generalized gradient approximations (GGAs), BLYP and PBE and four hybrid density functionals (B3LYP,[38−41] B97,[62] PBE0[63,64] and PW6B95,[65] which contain 20, 19.43, 25 and 28% "exact" exchange), several "modern" functionals are included in the benchmark:

The double hybrid B2PLYP[66] contains 53% "exact" exchange and 27% MBPT2 correlation energy, partially accounting for weak interactions. Nevertheless, for general applications a posteriori dispersion corrections have been recommended, denoted by appending -D (= -D2),[67] -D3[19] and -D3(BJ).[68]

The long-range corrected (LC) exchange functionals are motivated by the incorrect decay of the potential of standard DFT functionals (the $xc$ potential of semilocal functionals decays exponentially along with the density, while the asymptotic form of the exact potential is $-1/r$). The overly rapid decay is held responsible for the delocalization error, causing the overstabilization of fractionally charged fragments.[69] Long-range corrected exchange functionals lead to the correct asymptotic potential and have been shown to reduce the delocalization error significantly.[26,70]

The long-range correction to exchange is introduced through the range-separation scheme pioneered by Savin et al. for combining multideterminantal methods with DFT approaches.[71,72] The most common choice is an Ewald-style partitioning of the electron repulsion operator $1/r_{12}$ to define the short- and long-range (SR and LR, respectively)

$$\frac{1}{r_{12}} = \underbrace{\frac{\mathrm{erfc}(\mu r_{12})}{r_{12}}}_{\mathrm{SR}} + \underbrace{\frac{\mathrm{erf}(\mu r_{12})}{r_{12}}}_{\mathrm{LR}} \tag{5}$$

where the $\mu$ (or, equivalently, $\omega$) parameter is selected empirically and controls the definition of the two ranges. LC-BOP,[73,74] and LC-$\omega$PBE[75,76] (also known as LC-$\omega$PBE08) are long-range corrected functionals tested herein: the long-range is described by "exact" exchange and the short-range by DFT exchange.

M06-2X[77] is a flexible, carefully fitted highly empirical hybrid-meta-GGA functional (54% "exact" exchange and about 30 parameters), designed to describe main group elements and weak interactions accurately. The more recent Minnesota functional M11[78] follows the same spirit, but includes 100% long-range and 42.8% short-range "exact" exchange.

Dispersion is a nonlocal phenomenon, absent from standard density functionals.[10−13] Accounting for the nonlocal nature is computationally expensive, but reasonably practical schemes have been developed recently, such as VV10 tested herein functional.[79] Alternatively, a posteriori atom pairwise dispersion corrections have been shown to capture the essence of the dispersion interaction energies.[14−21] The general formula for such corrections is given by

$$E_{\mathrm{disp}} = -\sum_{i=2}^{N_{\mathrm{at}}} \sum_{j=1}^{i-1} f_d(R_{ij};\, i;\, j) \frac{C_6^{ij}}{R_{ij}^6} \tag{6}$$

where $N_{\mathrm{at}}$ is the number of atoms, $C_6^{ij}$ is the dispersion coefficient between atom $i$ and $j$, and $f_{\mathrm{d}}(R_{ij};i;j)$ is the damping function, which has to remove the divergence at zero internuclear distance $R_{ij}$. Furthermore, $f_{\mathrm{d}}$ adapts the dispersion correction to a given functional. In "classical" dispersion corrections, the dispersion coefficients are fixed parameters and the damping function depends on tabulated van der Waals radii.[14,16] To improve the accuracy, dependence on the geometry[19] or, even more general, on the electron density have been developed.[15,17,18,20] Two density dependent variants are tested: our recently introduced dispersion correction dDsC[20−22] and the local response dispersion (LRD) scheme of Sato and Nakai.[17,80] Note that both density dependent dispersion energy corrections are applied a posteriori; that is, they do not influence the electron density.

Combining a long-range corrected exchange functional with a dispersion correction is expected to lead to generally robust functionals, even though some combinations are known to be problematic.[20,24,81] Herein, we test LC-$\omega$PBE ($\omega$ = 0.45 bohr$^{-1}$)[75,76] together with our density dependent dispersion correction dDsC and either PBE, LYP,[38] or B95[82] correlation, leading to LC-$\omega$PBE-dDsC, LC-$\omega$PBELYP-dDsC, and LC-$\omega$PBEB95-dDsC. PBE correlation is the "natural" choice, but LYP and B95 are one-electron self-interaction free and might therefore offer some further reduction of the delocalization error. Alternatively to dDsC, LC-$\omega$PBE is combined with Vydrov and Van Voorhis' fully nonlocal correlation functional, denoted by LC-VV10.[79,83] Similarly, LC-BOP-LRD corrects LC-BOP with the local response dispersion (LRD) method of Sato and Nakai.[17,80] Finally, $\omega$B97X-D combines a highly fitted, long-range corrected functional with a "classical" dispersion correction.[84]

In summary, five different variants of long-range corrected exchange functionals that should also account for weak interactions are assessed: an empirical but specifically adapted exchange-correlation functional (M11),[78] an empirical exchange-correlation functional fitted together with an empirical "classical" dispersion correction ($\omega$B97X-D),[84] and three different density dependent dispersion corrections applied to long-range corrected exchange functionals that have not been specifically refitted (dDsC,[20] the local response formalism (LRD),[17,80] and the fully nonlocal VV10 functional[79]).

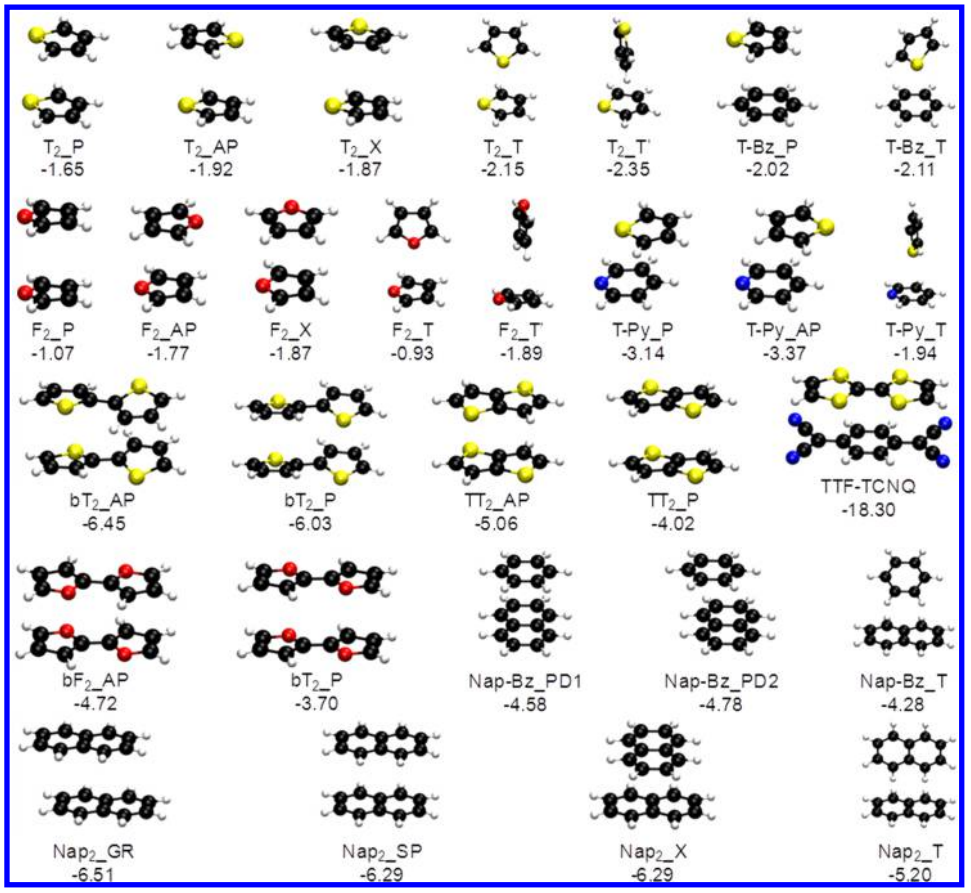


**Figure 1.** Pi29n test set with estimated CCSD(T)/CBS interaction energies in kcal mol$^{-1}$.

All DFT computations are run in a development version of Q-Chem,[85] except LC-BOP-LRD,[17,80] which is performed in GAMESS.[86] LC-BOP-LRD[10,0] refers to LC-BOP-LRD without the multicenter corrections to the $C_6$ coefficients introduced in ref 80. For benchmarking purposes, the large def2-QZVP(-g)[87] basis set has been applied. For testing a level more likely to be used in "real life" applications, selected data is also provided with the small 6-31G* and medium sized 6-311+G** basis sets. The integral threshold was set to $10^{-12}$, and a 75/305 Euler–Maclaurin–Lebedev[88,89] grid was used for most computations, but for M06-2X[77] and M11,[78] the finer 99/590 grid was adopted. The nonlocal part of the VV10[79] functional and all 6-31G* computations exploited the efficient SG-1 grid.[90] B2PLYP[66] computations were accelerated by the resolution of identity with the auxiliary basis set of aug-cc-pVTZ.[91] DFT computations are not corrected for the BSSE, and open-shell systems were treated in the unrestricted formalism. For several of the radical cation $\pi$-dimers, the identification of the lowest energy SCF solution was difficult for long-range corrected functionals, even around equilibrium.

## RESULTS AND DISCUSSION

**Test Sets.** This subsection introduces the test sets and discusses general trends based on the reference interaction energies (estimated CCSD(T)/CBS).

The Pi29n test set consists of a selection of weakly polar, neutral stacked, and T-shaped $\pi$-dimers including 15 sulfur-containing complexes (i.e., thiophene, thienothiophene, and bithiophene). Pi29n is representative of the "resting state" of organic electronics, which are not well represented in other test sets (e.g., PPS5/05[65] and S22[37]). The dimers are illustrated in Figure 1 with their abbreviations explained in Table 1. Due to the absence of hydrogen bonds, the interaction energies probed by Pi29n are dominated by dispersion. Nevertheless, electrostatic (e.g., dipole–dipole) and charge-transfer (donor–acceptor) interactions modulate the strength of the dispersion interactions by influencing the intermolecular separation (vide infra). The test set also contains two weak (thiophene···pyridine) and one strong (TTF-TCNQ) donor–acceptor complexes. Instead of the typical benzene dimer included in several test sets (e.g., PPS5/05[65] and S22[37]), the interactions between unsaturated hydrocarbons are here illustrated by the benzene···naphthalene and naphthalene dimers.

In line with the benzene dimer, the T-shaped thiophene dimer is more favorable (by about 0.4 kcal mol$^{-1}$) than the sandwich conformation, independently from the alignment of the molecular dipoles (parallel vs antiparallel), which was already noted by Tsuzuki et al.[34] The interaction energies of the furan dimers follow the same trends, with the exception of $F_2$_T, which is the least stable orientation, presumably due to the lower polarizability of the oxygen atom as compared to sulfur. The stacked thiophene···benzene dimer has essentially the same interaction energy as the antiparallel stacked thiophene dimer (~2 kcal mol$^{-1}$, slightly larger than the 1.7 kcal mol$^{-1}$ for stacked benzene dimer[92]). The interaction energy of thiophene···pyridine is substantially higher (~3 kcal mol$^{-1}$) and this also in comparison with the parallel displaced benzene dimer (~2.7 kcal mo$^{l-}$1).[92] The increasing interaction energy going from the thiophene dimer to thiophene···pyridine can be easily rationalized by the weak donor–acceptor ability of

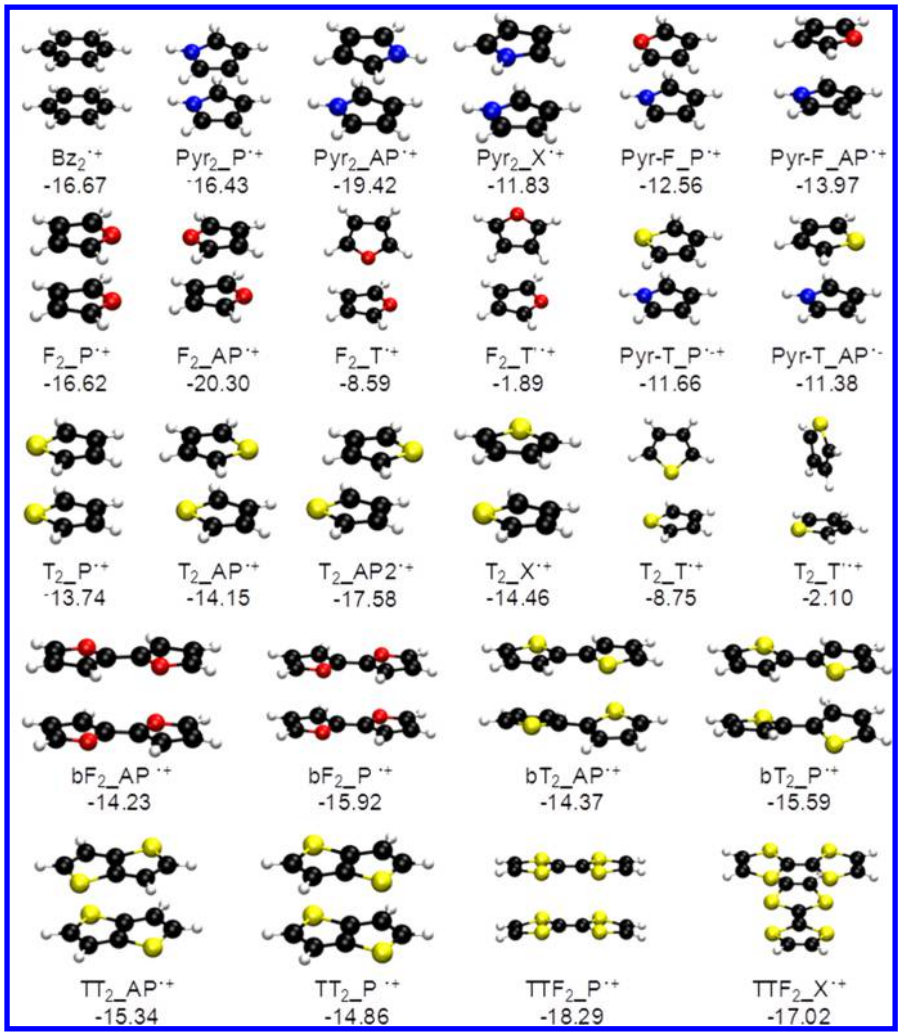


**Figure 2.** Orel26rad test set with estimated CCSD(T)/CBS interaction energies in kcal mol$^{-1}$.

the electron rich thiophene and the electron poor pyridine. This charge-transfer interaction reduces the intermolecular distance from ∼4.0 to 3.5 Å and concurrently leads to an augmentation of the dispersion interactions in the complex similar to TTF-TCNQ.[24]

Complexes involving larger monomers such as bifuran, thienothiophene, bithiophene, and naphthalene are bound more strongly due to the increase in dispersion interactions. The main interaction energy of 6.5 kcal mol$^{-1}$ is achieved for the antiparallel bithiophene dimer ($bT_2$_AP) and the graphite like naphthalene dimer ($Nap_2$_GR). The less polarizable bifuran dimers are bound less strongly (4.7 kcal mol$^{-1}$ for $bF_2$_AP). Alternatively, the T-shaped dimers are destabilized with respect to parallel displaced geometries when increasing the monomer size: the two types of benzene dimers are essentially isoenergetic (2.7 kcal mol$^{-1}$),[92] the parallel displaced benzene···naphthalene is slightly favored over the T-shaped (4.8 vs 4.3 kcal mol$^{-1}$), whereas the energy difference is larger than 1 kcal mol$^{-1}$ (5.2 vs 6.5 kcal mol$^{-1}$) for naphthalene dimers. The prototypical charge-transfer complex TTF-TCNQ has, by far, the largest interaction energy ($\Delta E$ = 18.2 kcal mol$^{-1}$).

This study's largest emphasis is placed on the radical cationic $\pi$-dimers (see Figure 2). In contrast to the neutral Pi29n complexes, the dimer radical cations are not only bound by dispersion but characterized by significant electrostatic, polarization, and charge-resonance (similar to the charge-transfer in case of the neutral monomers and also sometimes referred to as "covalent-like") interactions typical of ion···neutral complexes. The relative orientation of the two monomers is determinant for the charge-resonance: the better the orbital overlap of the HOMO/SOMO, the more stabilized is the complex.

To span a representative range of monomers commonly employed in p-doped organic polymers, we selected a set of homo- and heterodimers of pyrrole, furan, and thiophene. The benzene dimer radical cation represents the most investigated species of its kind[93−99] and is also included in the test set. The more extended bithiophene, bifuran, thienothiophene, and TTF mixed valence dimers provide more realistic models of organic electronics precursors.

The antiparallel pyrrole and furan dimer radical cations ($Pyr_2$_$AP^{\bullet+}$ and $F_2$_$AP^{\bullet+}$) are the most strongly bound complexes (about 20 kcal mol$^{-1}$) of Orel26rad. This strong interaction energy is best explained by the optimum monomer orbital alignment (along the C═C double bonds) that leads to the bonding SOMOs in the dimer radical cations. The interaction energies of these "special" dimers ($Pyr_2$_$AP^{\bullet+}$ and $F_2$_$AP^{\bullet+}$) are matched closely only by the significantly larger TTF dimer radical cations (17 and 18 kcal mol$^{-1}$ for the cross and parallel orientation, respectively). The antiparallel thio-


dx.doi.org/10.1021/ct300657h | J. Chem. Theory Comput. 2012, 8, 4305−4316

phene radical cation dimer ($T_2$_$AP^{\bullet+}$) is bound by about 14 kcal mol$^{-1}$, which is 2.5 kcal mol$^{-1}$ less than the benzene dimer radical cation and significantly less than $Pyr_2$_$AP^{\bullet+}$ and $F_2$_$AP^{\bullet+}$. It is worthwhile to note that since sulfur is larger than oxygen, the intermolecular distance is increased in $T_2$_$AP^{\bullet+}$ relative to $F_2$_$AP^{\bullet+}$ (3.2 vs 2.9 Å). The amount of Pauli repulsion is reduced in the lateral displaced arrangement as the sulfur lies above the "empty" region between the two hydrogen atoms ($T_2$_$AP2^{\bullet+}$ in Figure 3). In the latter

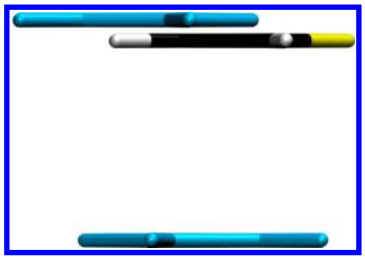

**Figure 3.** Comparison of $T_2$_$AP^{\bullet+}$ in cyan and $T_2$_$AP2^{\bullet+}$.

arrangement, the two thiophene monomers are closer to each other (2.9 Å), resulting in an increased interaction energy from 14.2 to 17.6 kcal mol$^{-1}$ for $T_2$_$AP^{\bullet+}$ and $T_2$_$AP2^{\bullet+}$, respectively.

The larger antiparallel bithiophene radical cation dimer, $bT_2$_$AP^{\bullet+}$, is bound by only 14 kcal mol$^{-1}$, as the bonding orbital is more extended and, therefore, less stabilizing. Apparently, the increase in dispersion interactions is slower than the loss in charge-resonance energy when increasing the monomer size. Thus, for the relatively small dimer radical cations studied here, variations in charge-resonance dominate over the change in dispersion interactions. For larger monomers (e.g., oligothiophenes), however, we expect that dispersion will eventually become more important for the total interaction energy, with charge-resonance contribution playing a diminishing role.

The T-shaped radical cation dimers do not benefit from significant orbital overlap (i.e., "covalent" interactions) and thus have smaller interaction energies of ∼9 kcal mol$^{-1}$. This energy range is only slightly below that of stacked complexes for which the charge resonance is weak (11−14 kcal mol$^{-1}$), either because of the different ionization energies of the two monomers (e.g., thiophene···pyrrole) or because of the nonbonding SOMO (e.g., the cross conformation of the pyrrole dimer, $Pyr_2$_$X^{\bullet+}$). The interaction energy is, however, much weaker (only ∼2 kcal mol$^{-1}$) when the heteroatom is pointing away from the second monomer (T′ orientation); that is, $\Delta E$ is similar to that of the neutral T-shaped complexes, which indicates that the pure electrostatic interaction (ion···neutral) and charge resonance are of minor importance in T′.

**Performance of Standard Wave Function Methods.** Interaction energies for the two test sets, Pi29n and Orel26rad, are given in Figures 4 and 5 at standard ab initio levels (see Table 2 for mean absolute deviations, MADs): MP2 at the complete basis set limit together with MP2 and CCSD(T) in the small basis set, 6-31G*(0.25). With a MAD of 0.3 kcal mol$^{-1}$, MP2/6-31G*(0.25) clearly outperforms MP2/CBS and CCSD(T)/6-31G*(0.25) (MADs of 2.0 and 2.1 kcal mol$^{-1}$, respectively) for the neutral $\pi$-dimers of the Pi29n test set. The relative performance is very similar for the more challenging Orel26rad test set with a MAD of 0.7 kcal mol$^{-1}$ for MP2/6-

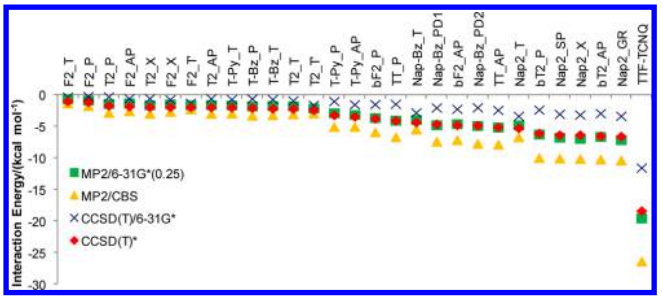


**Figure 4.** Ab inito interaction energies in kcal mol$^{-1}$ for the Pi29n test set. CCSD(T)* denotes the estimated CCSD(T)/CBS values serving as the benchmark.

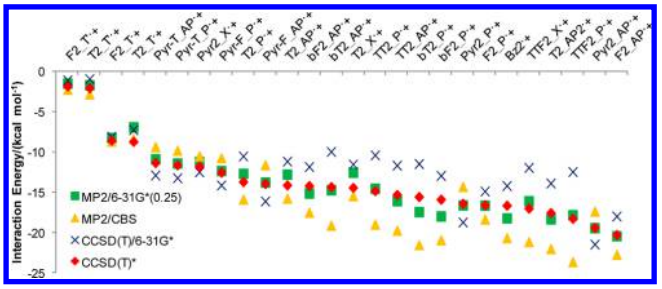


**Figure 5.** Ab inito interaction energies in kcal mol$^{-1}$ for the Orel26rad test set. CCSD(T)* denotes the estimated CCSD(T)/CBS values and serves as the benchmark.

31G*(0.25) compared to MADs of 2.7 and 2.6 kcal mol$^{-1}$ for the two much more demanding wave function methods. The remarkable performance of MP2/6-31G*(0.25) is in line with previous studies reporting the reliable accuracy of this cost-effective combination[46,100,101] due to error cancellation: MP2/CBS tends to overestimate interactions between $\pi$-conjugated molecules, while smaller basis sets limit the flexibility of the wave function and therefore lead to less binding. However, such an error cancellation does not hold for more accurate theories (e.g., CCSD(T)) for which weak interactions are underestimated in small basis sets.

With an overall MAD of 0.5 kcal mol$^{-1}$, MP2/6-31G*(0.25) emerges as the most accurate approximate level of theory discussed herein, outperforming all tested density functional approximations.

**Performance of Density Functional Approximations.** Despite the remarkable success of MP2/6-31G*(0.25), the performance of density functional approximations (Figure 6) is of considerable interest for general applications and for understanding the limitations of current approaches.

Simple PBE-dDsC achieves an impressive MAD of only 0.5 kcal mol$^{-1}$ for Pi29n with many other dispersion corrected functionals providing an excellent accuracy, as illustrated by the performance of VV10 (MAD = 0.1 kcal mol$^{-1}$). The success of dispersion corrected functionals for Pi29n indicates good transferability from the smaller complexes dominating most training sets for weak interactions (e.g., S22) to the larger and sulfur containing complexes of Pi29n. In other words, as long as dispersion is accounted for, neutral model complexes of organic electronics are not problematic.

The description of Orel26rad is more delicate. GGA functionals (BLYP and PBE) are among the worst methods tested (averaged MAD of 6.7 and 4.7 kcal mol$^{-1}$) but have a lower MAD for Orel26rad than for Pi29n due to error cancellation between overestimated charge-delocalization and

**Table 2. Performance of Various Methods for the Two Individual Test Sets and the Average MAD[a]**

| | Orel26rad | Pi29n | avg. MAD |
|---|---|---|---|
| HF | 17.31 | 7.79 | 12.29 |
| LC-BOP | 9.94 | 5.31 | 7.50 |
| LC-$\omega$PBE | 9.14 | 4.92 | 6.92 |
| LC-$\omega$PBELYP | 9.33 | 4.33 | 6.69 |
| BLYP | 5.67 | 7.56 | 6.67 |
| B3LYP | 5.91 | 6.62 | 6.28 |
| B97 | 4.79 | 5.50 | 5.16 |
| PBE | 4.58 | 4.82 | 4.70 |
| LC-$\omega$PBEB95 | 6.06 | 2.83 | 4.36 |
| PBE0 | 3.78 | 4.87 | 4.36 |
| PBE-dDsC | 7.52 | 0.51 | 3.82 |
| VV10 | 7.86 | 0.14 | 3.79 |
| BLYP-dDsC | 6.28 | 1.25 | 3.63 |
| HF-dDsC | 5.16 | 1.70 | 3.34 |
| PW6B95 | 2.93 | 3.50 | 3.23 |
| M11 | 3.36 | 1.82 | 2.55 |
| B2PLYP | 1.79 | 3.20 | 2.54 |
| LC-$\omega$PBE-dDsC | 4.26 | 0.97 | 2.53 |
| CCSD(T)/6-31G*(0.25) | 2.60 | 2.13 | 2.35 |
| MP2/CBS | 2.68 | 2.02 | 2.33 |
| PW6B95-dDsC | 4.16 | 0.60 | 2.28 |
| B3LYP-dDsC | 4.01 | 0.55 | 2.19 |
| B97-dDsC | 3.94 | 0.43 | 2.09 |
| LC-$\omega$PBELYP-dDsC | 3.76 | 0.41 | 1.99 |
| LC-$\omega$PBEB95-dDsC | 3.27 | 0.59 | 1.86 |
| PBE0-dDsC | 3.40 | 0.39 | 1.81 |
| B2PLYP-D3(BJ) | 3.26 | 0.42 | 1.76 |
| LC-VV10 | 3.12 | 0.39 | 1.68 |
| LC-BOP-LRD[10,0] | 3.17 | 0.21 | 1.61 |
| LC-BOP-LRD | 2.85 | 0.30 | 1.51 |
| B2PLYP-D | 2.74 | 0.35 | 1.48 |
| LC-$\omega$PBEB95-dDsC/6-31G* | 1.90 | 0.92 | 1.38 |
| B2PLYP-D3 | 2.61 | 0.21 | 1.35 |
| LC-$\omega$PBEB95-dDsC/6-311+G** | 1.78 | 0.82 | 1.27 |
| M06-2X | 1.08 | 1.25 | 1.16 |
| $\omega$B97X-D | 1.41 | 0.41 | 0.88 |
| MP2/6-31G*(0.25) | 0.74 | 0.33 | 0.52 |

[a]All energies are in kcal mol$^{-1}$.

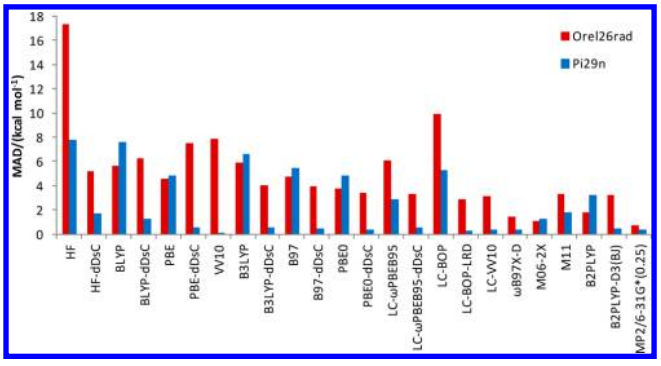


**Figure 6.** Performance of density functional approximations for radical cations (Orel26rad) and neutral $\pi$-dimers (Pi29n).

missing dispersion. Adding a dispersion energy correction to a GGA functional (i.e., BLYP-dDsC, PBE-dDsC), deteriorates the performance for Orel26rad of these functionals even further. The fully nonlocal VV10 functional is not better than PBE-dDsC and is therefore not recommended either.

Standard hybrid density functionals such as B3LYP or PBE0 show a slight improvement over GGAs (averaged MAD of 6.3 and 4.4 kcal mol$^{-1}$ for B3LYP and PBE0, respectively). With an average MAD of 1.8 kcal mol$^{-1}$, PBE0-dDsC is the best performing functional among the "simple" approaches. The other dispersion corrected hybrid functionals perform slightly worse, with average MADs of about 2.2 kcal mol$^{-1}$. These results demonstrate that the real benefit of including a fraction of "exact" exchange is only visible in combination with a dispersion energy correction. Alternatively, the highly empirical global hybrid meta-GGA functional M06-2X achieves an overall MAD of 1.2 kcal mol$^{-1}$, providing a balanced description of Orel26rad and Pi29n (MADs of 1.1 and 1.3 kcal mol$^{-1}$, respectively).

Similar to global hybrids, LC- variants of standard functionals (e.g., LC-$\omega$PBE or LC-BOP) do not perform well for either Pi29n or Orel26rad (MADs > 7 kcal mol$^{-1}$), illustrating again the importance of weak interactions for achieving quantitative agreement with benchmark data. The modest performance of M11 ($MAD_{Orel26rad}$ = 3.4 kcal mol$^{-1}$) indicates that the reduction of the delocalization error alters the error cancellation at the origin of the successful description of weak interactions by M06-2X (the global hybrid predecessor of M11). In other words, long-range corrected exchange necessitates the explicit treatment of dispersion interactions for achieving accurate energetics. Orel26rad benefits the most from simultaneously accounting for weak interaction and reducing the delocalization energy. However, only $\omega$B97X-D (MAD of 1.4 kcal mol$^{-1}$) reaches chemical accuracy (2 kcal mol$^{-1}$). In other words, the addition of a dispersion correction (dDsC, VV10 or LRD) to a standard LC- functional is not fully satisfactory and a better performance is achieved when fitting empirically the exchange-correlation functional together with the dispersion correction. LC-BOP-LRD is the best among the less empirical functionals, but the MAD of 2.9 kcal mol$^{-1}$ indicates that improvement is still possible.[102]

The most popular double hybrid functional, B2PLYP,[66] has been combined with the three successively recommended dispersion corrections: -D (=D2),[67] -D3,[19] and -D3(BJ).[68] With a MAD of 1.8 and 3.2 kcal mol$^{-1}$ for Orel26rad and Pi29n, respectively, plain B2PLYP satisfies the chemical accuracy criterion for Orel26rad, but not for the neutral complexes. Adding a dispersion correction improves the performance for Pi29n significantly (MAD of 0.2−0.4 kcal mol$^{-1}$), but the accuracy for the other test set is clearly affected, for example, the MAD for B2PLYP-D3 is 2.6 kcal mol$^{-1}$ for Orel26rad.

With average MADs of 1.2 and 0.9 kcal mol$^{-1}$, the best performing M06-2X and $\omega$B97X-D rival with the accuracy of MP2/6-31G*(0.25) (MAD = 0.6 kcal mol$^{-1}$). As compared to MP2, M06-2X has more difficulties describing the dispersion-dominated complexes ($MAD_{Pi29n}$ = 1.3 vs 0.3 kcal mol$^{-1}$, for M06-2X and MP2, respectively), whereas Orel26rad is trickier for $\omega$B97X-D (MAD = 1.4 and 0.7 kcal mol$^{-1}$ for $\omega$B97X-D and MP2, respectively).

To summarize, interaction energies of radical cation $\pi$-dimers as illustrated by the Orel26rad test set are especially challenging: the electronic structure is more complicated than for the neutral dimers of Pi29n and dispersion interactions are still important. The carefully fitted M06-2X, which performs very well, exploits the error cancellation between the missing dispersion and the delocalization error. Without relying on such delicate error cancellations, only $\omega$B97X-D adequately

describes interaction energies of both neutral and radical cations. The reduction of the delocalization error in ωB97X-D is, however, associated with the fitting of the (exchange-correlation) functional augmented by an explicit dispersion correction.

The MAD is a good indicator of the overall accuracy, but capturing trends is sometimes more relevant than reproducing absolute binding energies. In particular, achieving the correct relative interactions between a series of complexes is of interest for identifying potential next-generation molecular precursors to organic electronics. The extent to which these trends are reproduced is analyzed on a subset of Orel26rad given in Figure 7. In contrast to Pi29n, for which the correlation between

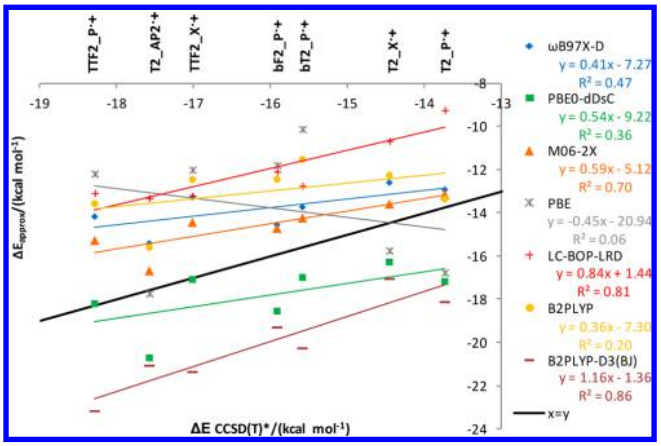


**Figure 7.** Correlation between DFT and estimated CCSD(T)/CBS interaction energies for a parallel and crossed TTF, bithiophene, bifuran dimers from Orel26rad test set (see the Supporting Information for the correlation graph showing the full Orel26rad test set).

dispersion corrected functionals and CCSD(T)* is rather good, Orel26rad is more problematic (see the Supporting Information for the full correlation plot). Neither B2PLYP (which neglects ∼50% of the dispersion) nor dispersion corrected density functionals clearly discriminate between the two $TTF_2^{\bullet+}$ complexes and the parallel thiophene cation dimer ($T_2$_$P^{\bullet+}$). Only B2PLYP-D3(BJ), which systematically overbinds the series, reproduces the 4.6 kcal mol$^{-1}$ energy spread between the parallel TTF ($TTF_2$_$P^{\bullet+}$) and $T_2$_$P^{\bullet+}$. The improvement of B2PLYP-D3(BJ) upon B2PLYP is rationalized by the proper treatment of dispersion interactions dominating the binding energy of the larger dimers.

The negative slope of PBE indicates that the delocalization error affects smaller systems more than extended ones: in larger monomers, the charge is more delocalized so that further spreading is not as advantageous. The "artificially" good performance of PBE for the smaller dimers (due to the larger delocalization error and missing dispersion) is, therefore, not effective for the larger systems, which are significantly underbound in the absence of dispersion correction.

In line with the MADs discussed above, the reduction of the delocalization error together with the description of dispersion interactions leads to a dramatic improvement going from PBE to PBE0-dDsC or ωB97X-D. Nevertheless, given that neither HF (the slope of the linear regression is zero, see the Supporting Information) nor pure GGAs (negative slope, e.g., PBE) contain the right physics to stabilize the larger systems more than the smaller ones, their linear combination (i.e., global hybrids) is not an ideal basis for a dispersion correction. Long-range corrected exchange together with a dispersion correction can provide more reasonable slopes, but the trends are not necessarily consistent (e.g., ωB97X-D vs LC-BOP-LRD). B2PLYP performs somewhat better, because the negative slope of the GGA component is counterbalanced by the fraction correlation energy from perturbation theory.

Overall, achieving the correct balance between the decrease of charge resonance and the gain in dispersion interactions in larger dimers is highly challenging. In particular, the approximations giving the most accurate binding energies (e.g., ωB97X-D and M06-2X) do not accurately reproduce the relative strength of a series of dimers.

**Interaction Energy Profiles.** The reproduction of interaction energy profiles certainly represents the most rigorous validation for identifying robustly methods. Non-equilibrium geometries are especially relevant in the context of molecular dynamics simulations. Interaction energy profiles are computed for the antiparallel furan and thiophene dimer radical cations ($F_2$_$AP^{\bullet+}$ and $T_2$_$AP^{\bullet+}$), two prototypical examples of organic charge-carriers. The comparison of the two profiles is convenient because despite their similar structures their interaction energy differs by about 6 kcal mol$^{-1}$.

The interaction energy profiles are computed on the basis of the respective dimers of the Orel26rad test set ($F_2$_$AP^{\bullet+}$ and $T_2$_$AP^{\bullet+}$); that is, one monomer corresponds to the optimized neutral and the other one to the radical cation geometry at the B3LYP/6-31G* level. The asymmetric nature of the dimers aims at improving the dissociation of the dimers: Density functional approximations are more accurate for integer than for fractional numbers of electrons. Charge-localization induced by a geometrical bias is expected to disfavor the symmetric solution with two monomers charged +0.5. The energy profiles of the symmetric dimers (i.e., fully optimized) are given in the Supporting Information.

Symmetry adapted perturbation theory,[55] allows, in principle, the identification of the origin of the interaction energies. Unfortunately, SAPT is far less developed for open-shell than for closed-shell complexes. Therefore, only the simplest variant, SAPT0, is applied herein in which the monomers are treated at the (RO)HF level and electron correlation is neglected except for the dispersion energy.

Akin to the equilibrium interaction energies, MP2/6-31G*(0.25) is in excellent agreement with CCSD(T)/CBS, whereas MP2/CBS overbinds the radical cation dimers of furan and thiophene (Figure 8). In contrast, SAPT0 accounts for only ∼50% of the CCSD(T)* interaction energy. More importantly, the difference between furan and thiophene is not reproduced. This qualitative failure is not surprising, considering that charge-resonance is important in these dimers and that SAPT is based on one charged and one neutral monomer. Adding the δHF term to SAPT0, which corresponds to Hartree−Fock supplemented by the SAPT dispersion energy (HF+Disp), leads to a qualitative improvement. However, the remaining errors of ∼4 kcal mol$^{-1}$ around equilibrium, indicates that HF +Disp is not in quantitative agreement with either CCSD(T)* or MP2/6-31G*(0.25).[103] In summary, the SAPT0 analysis confirms the importance of charge-resonance (i.e., δHF is essential for the qualitative agreement) and dispersion interactions. However, correlation contributions beyond "simple" monomer-based dispersion (e.g., induction-dispersion) are expected to be non-negligible for these strongly interacting monomers: The monomer densities at the basis of

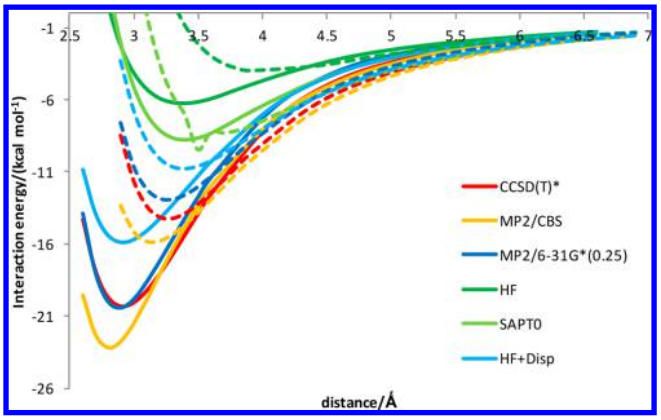


**Figure 8.** Interaction energy profiles for the radical cation dimers of furan (solid line) and thiophene (broken lines) at various levels of theory. SAPT0 is performed in the small 6-31G*(0.25) basis set and HF+Disp refers to the Hartree−Fock interaction energy augmented by the SAPT0 dispersion energy. The "discontinuous" point of SAPT0 for the thiophene dimer corresponds to the maximum net stabilization due to induction. It is probably an artifact from the perturbative treatment (e.g., eq 4); note that, at this intermolecular distance, electrostatic attraction is still dominated by exchange repulsion.

the SAPT0 treatment are only a very rough approximation to the dimer densities.

The overall performance of the DFT approximations is rather poor (Figure 9): the qualitative difference between the

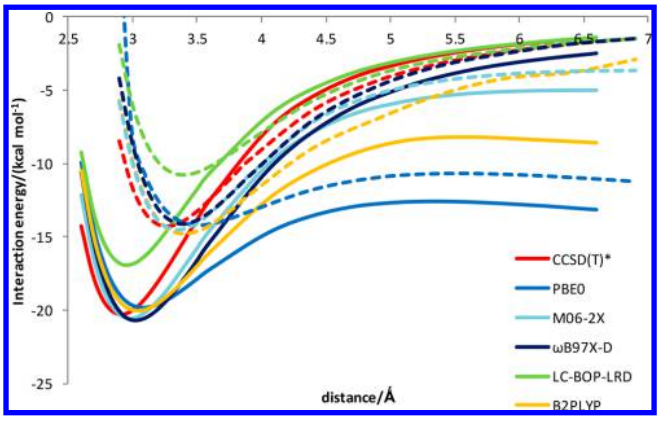


**Figure 9.** Interaction energy profiles for the radical cation dimers of furan (solid line) and thiophene (broken lines) at various DFT levels compared to estimated CCSD(T)/CBS.

furan and thiophene dimer radical cations is adequately reproduced, but only ωB97X-D provides both accurate binding energies and correct dissociation behavior. The other long-range corrected exchange functionals (including LC-ωPBEB95-dDsC, see Supporting Information) perform very similarly to each other and underestimate the interaction energy by about 3 kcal mol$^{-1}$ (as also apparent in their MAD for Orel26rad). The equilibrium distance is nevertheless accurate to within ±0.1 Å for all the LC- functionals. Finally, the wrong dissociation behavior of M06-2X contrasts with the low MAD for Orel26rad (1.1 kcal mol$^{-1}$). However, the high amount of "exact" exchange in M06-2X reduces the delocalization error sufficiently to remove the spurious barriers toward dissociation obtained with other functionals (e.g., furan dimer radical cation with PBE0 and B2PLYP).

**Basis Set Dependence.** Large basis sets are necessary to assess the "true" functional performance, but quadruple-ζ basis sets are not realistic for routine applications. We here compare the performance of two standard, economic basis sets with that of def2-QZVP(-g) using the best dDsC corrected variant, that is, the long-range corrected functional, LC-ωPBEB95-dDsC (Figure 10). The average MADs over all the interaction

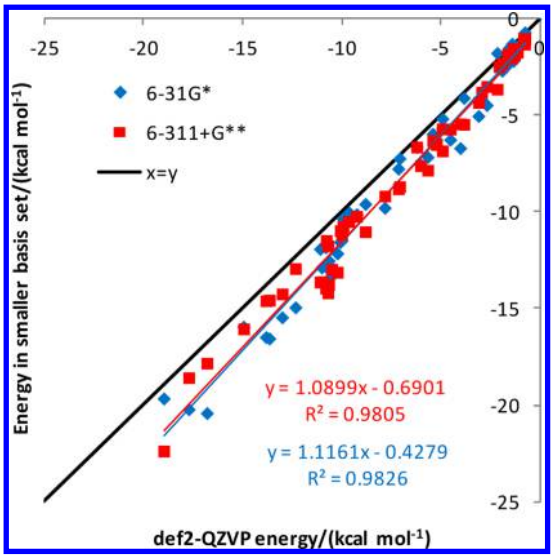


**Figure 10.** Correlation between interaction energies in smaller basis sets (6-31G* and 6-311+G**) and def2-QZVP(-g) values for the LC-ωPBEB95-dDsC density functional.

energies are 1.4, 1.3, and 1.9 kcal mol$^{-1}$ for 6-31G*, 6-311+G**, and def2-QZVP(-g), respectively. The use of the LC-ωPBEB95-dDsC/6-31G* combination, in future application, is justified by the small difference between 6-31G* and 6-311+G** and by the reasonable accuracy of the most cost-efficient variant tested herein. In fact, the average MAD is lower when using the small basis sets: the underbinding of LC-ωPBEB95-dDsC is compensated by the basis set superposition error (average MADs of 1.4 and 1.9 kcal mol$^{-1}$ for 6-31G* and def2-QZVP(-g), respectively).

## CONCLUSIONS

The accurate computational description of molecular precursors to organic electronics may promote our ability to address the most relevant questions in the field. With the aim of assessing the performance of the most accessible electronic structure methods for relevant interaction energies, we have introduced two test sets composed of neutral and radical dimer complexes, which best represent the resting (Pi29n) and charge-carrier states (Orel26rad) of organic functional units. The description of the interaction energies of neutral complexes (Pi29n) is straightforward, so long as dispersion interactions are properly taken into account: the best performing combinations are MP2/6-31G*(0.25), B2PLYP-D3, LC-BOP-LRD, and VV10, as well as the less demanding PBE0-dDsC. In contrast, these approaches give results greatly exceeding chemical accuracy for the Orel26rad test set, with the exception of MP2/6-31G*(0.25), which clearly outperforms all other tested schemes. Achieving interplay between reducing charge delocalization and accounting for dispersion interactions in π-dimer radical cations is highly challenging for density functional approximations. For equilibrium geometries, M06-


dx.doi.org/10.1021/ct300657h | J. Chem. Theory Comput. 2012, 8, 4305−4316

2X and ωB97X-D best reproduce the binding energies (MAD of 1.1 and 1.4 kcal $mol^{-1}$, respectively) of the charged radical complexes. The inclusion of long-range corrected exchange requires explicit treatment of dispersion interactions yet, with the exception of ωB97X-D, the performance of the LC- family of functionals is disappointing due to the systematic underestimation of the binding energy. The advantage of the long-range corrected formalism is nevertheless significant, particularly when energy profiles are considered. The correct dissociation behavior of a dimer into one charged and one neutral monomer is achieved only with functionals possessing the correct form in the asymptotic region. In addition, the underestimation of interaction energies at the equilibrium distance can be compensated by the basis set superposition error when using a small, more practical basis sets.

Overall, the dilemma between reproducing absolute binding energies, relative energy trends, and dissociation behavior suggests that MP2/6-31G*(0.25) is the best approximation. When dealing with "real-world" applications involving larger systems, the description of Orel26rad is subtle; our findings indicate that the use of dispersion corrected long-range functionals together with a small double-ζ basis set (e.g., LC-ωPBEB95-dDsC/6-31G*) represent the most cost-effective and promising alternative. The challenging Orel26rad database can function as a valuable test set used to develop improved schemes.

## ■ ASSOCIATED CONTENT

### Supporting Information

Geometries of all monomers and dimers published in this work, together with reference interaction energies and interaction energies for all approximate methods tested. Additional figures provide interaction energy profiles for symmetric furan and thiophene dimer radical cations and correlation plots between CCSD(T)* and DFT methods for the Pi29n and Orel26rad test sets. This material is available free of charge via the Internet at http://pubs.acs.org.

## ■ AUTHOR INFORMATION

### Corresponding Author

*E-mail: clemence.corminboeuf@epfl.ch; stephan.steinmann@epfl.ch.

### Notes

The authors declare no competing financial interest.

## ■ ACKNOWLEDGMENTS

C.C. acknowledges the Sandoz family foundation, the Swiss NSF Grant 200021_121577/1, and EPFL for financial support. We are grateful to Q-Chem Inc. for providing the source code of Q-Chem.

## ■ DEDICATION

C.C. dedicates this paper to the memory of a great mentor, Jacques Weber.

## ■ REFERENCES

(1) Gunes, S.; Neugebauer, H.; Sariciftci, N. S. *Chem. Rev.* **2007**, *107*, 1324−1338.
(2) Walzer, K.; Maennig, B.; Pfeiffer, M.; Leo, K. *Chem. Rev.* **2007**, *107*, 1233−1271.
(3) Allard, S.; Forster, M.; Souharce, B.; Thiem, H.; Scherf, U. *Angew. Chem., Int. Ed.* **2008**, *47*, 4070−4098.
(4) Sauvage, J.-P. *Acc. Chem. Res.* **1998**, *31*, 611−619.
(5) Joachim, C.; Gimzewski, J. K.; Aviram, A. *Nature* **2000**, *408*, 541−548.
(6) Pease, A. R.; Jeppesen, J. O.; Stoddart, J. F.; Luo, Y.; Collier, C. P.; Heath, J. R. *Acc. Chem. Res.* **2001**, *34*, 433−444.
(7) Kinbara, K.; Aida, T. *Chem. Rev.* **2005**, *105*, 1377−1400.
(8) Kay, E. R.; Leigh, D. A.; Zerbetto, F. *Angew. Chem., Int. Ed.* **2007**, *46*, 72−191.
(9) Kohn, W.; Sham, L. J. *Phys. Rev.* **1965**, *140*, A1133−A1138.
(10) Kristyan, S.; Pulay, P. *Chem. Phys. Lett.* **1994**, *229*, 175−180.
(11) Perez-Jorda, J. M.; Becke, A. D. *Chem. Phys. Lett.* **1995**, *233*, 134−137.
(12) Hobza, P.; Sponer, J.; Reschel, T. *J. Comput. Chem.* **1995**, *16*, 1315−1325.
(13) Zhang, Y.; Pan, W.; Yang, W. *J. Chem. Phys.* **1997**, *107*, 7921−7925.
(14) Wu, Q.; Yang, W. *J. Chem. Phys.* **2002**, *116*, 515−524.
(15) Johnson, E. R.; Becke, A. D. *J. Chem. Phys.* **2006**, *124*, 174104.
(16) Grimme, S. *J. Comput. Chem.* **2006**, *27*, 1787−1799.
(17) Sato, T.; Nakai, H. *J. Chem. Phys.* **2009**, *131*, 224104.
(18) Tkatchenko, A.; Scheffler, M. *Phys. Rev. Lett.* **2009**, *102*, 073005.
(19) Grimme, S.; Antony, J.; Ehrlich, S.; Krieg, H. *J. Chem. Phys.* **2010**, *132*, 154104.
(20) Steinmann, S. N.; Corminboeuf, C. *J. Chem. Theory Comput.* **2011**, *7*, 3567−3577.
(21) Steinmann, S. N.; Corminboeuf, C. *J. Chem. Theory Comput.* **2010**, *6*, 1990−2001.
(22) Steinmann, S. N.; Corminboeuf, C. *J. Chem. Phys.* **2011**, *134*, 044117.
(23) Steinmann, S. N.; Wodrich, M.; Corminboeuf, C. *Theor. Chem. Acc.* **2010**, *127*, 429−442.
(24) Steinmann, S. N.; Piemontesi, C.; Delachat, A.; Corminboeuf, C. *J. Chem. Theory Comput.* **2012**, *8*, 1629−1640.
(25) Zhang, Y.; Yang, W. *J. Chem. Phys.* **1998**, *109*, 2604−2608.
(26) Mori-Sanchez, P.; Cohen, A. J.; Yang, W. *J. Chem. Phys.* **2006**, *125*, 201102.
(27) Ruzsinszky, A.; Perdew, J. P.; Csonka, G. I.; Vydrov, O. A.; Scuseria, G. E. *J. Chem. Phys.* **2006**, *125*, 194112.
(28) Ruzsinszky, A.; Perdew, J. P.; Csonka, G. I.; Vydrov, O. A.; Scuseria, G. E. *J. Chem. Phys.* **2007**, *126*, 104102−8.
(29) Novoa, J. J.; Lafuente, P.; Del Sesto, R. E.; Miller, J. S. *Angew. Chem., Int. Ed.* **2001**, *40*, 2540−2545.
(30) Cohen, A. J.; Mori-Sanchez, P.; Yang, W. *J. Chem. Phys.* **2008**, *129*, 121104.
(31) Jakowski, J.; Simons, J. *J. Am. Chem. Soc.* **2003**, *125*, 16089−16096.
(32) Jung, Y.; Head-Gordon, M. *Phys. Chem. Chem. Phys.* **2004**, *6*, 2008−2011.
(33) García-Yoldi, I.; Mota, F.; Novoa, J. J. *J. Comput. Chem.* **2007**, *28*, 326−334.
(34) Tsuzuki, S.; Honda, K.; Azumi, R. *J. Am. Chem. Soc.* **2002**, *124*, 12200−12209.
(35) Podeszwa, R.; Szalewicz, K. *Phys. Chem. Chem. Phys.* **2008**, *10*, 2735−2746.
(36) Lee, N. K.; Park, S.; Kim, S. K. *J. Chem. Phys.* **2002**, *116*, 7902−7909.
(37) Jurecka, P.; Sponer, J.; Cerny, J.; Hobza, P. *Phys. Chem. Chem. Phys.* **2006**, *8*, 1985−1993.
(38) Lee, C.; Yang, W.; Parr, R. G. *Phys. Rev. B* **1988**, *37*, 785.
(39) Becke, A. D. *Phys. Rev. A* **1988**, *38*, 3098.
(40) Becke, A. D. *J. Chem. Phys.* **1993**, *98*, 5648−5652.
(41) Stephens, P. J.; Devlin, F. J.; Chabalowski, C. F.; Frisch, M. J. *J. Phys. Chem.* **1994**, *98*, 11623−11627.
(42) Frisch, M. J.; Trucks, G. W.; Schlegel, H. B.; Scuseria, G. E.; Robb, M. A.; Cheeseman, J. R.; Scalmani, G.; Barone, V.; Mennucci, B.; Petersson, G. A.; Nakatsuji, H.; Caricato, M.; Li, X.; Hratchian, H. P.; Izmaylov, A. F.; Bloino, J.; Zheng, G.; Sonnenberg, J. L.; Hada, M.; Ehara, M.; Toyota, K.; Fukuda, R.; Hasegawa, J.; Ishida, M.; Nakajima, T.; Honda, Y.; Kitao, O.; Nakai, H.; Vreven, T.; Montgomery, J. A., Jr.; Peralta, J. E.; Ogliaro, F.; Bearpark, M.; Heyd, J. J.; Brothers, E.; Kudin,

K. N.; Staroverov, V. N.; Kobayashi, R.; Normand, J.; Raghavachari, K.; Rendell, A.; Burant, J. C.; Iyengar, S. S.; Tomasi, J.; Cossi, M.; Rega, N.; Millam, J. M.; Klene, M.; Knox, J. E.; Cross, J. B.; Bakken, V.; Adamo, C.; Jaramillo, J.; Gomperts, R.; Stratmann, R. E.; Yazyev, O.; Austin, A. J.; Cammi, R.; Pomelli, C.; Ochterski, J. W.; Martin, R. L.; Morokuma, K.; Zakrzewski, V. G.; Voth, G. A.; Salvador, P.; Dannenberg, J. J.; Dapprich, S.; Daniels, A. D.; Farkas, O.; Foresman, J. B.; Ortiz, J. V.; Cioslowski, J.; Fox, D. J. *Gaussian 09, Revision A.1*; Gaussian, Inc.: Wallingford, CT, 2009.

(43) Werner, H.-J.; Manby, F. R.; Knowles, P. J. *J. Chem. Phys.* **2003**, *118*, 8149−8160.

(44) Helgaker, T.; Klopper, W.; Koch, H.; Noga, J. *J. Chem. Phys.* **1997**, *106*, 9639−9646.

(45) Kroon-Batenburg, L. M. J.; van Duijneveldt, F. B. *J. Mol. Struct. Theochem* **1985**, *121*, 185−199.

(46) Hobza, P.; Sponer, J. *Chem. Rev.* **1999**, *99*, 3247−3276.

(47) Boys, S. F.; Bernardi, F. *Mol. Phys.* **1970**, *19*, 553−566.

(48) Werner, H.-J.; Knowles, P. J.; Lindh, R.; Manby, F. R.; Schütz, M.; Celani, P.; Korona, T.; Mitrushenkov, A.; Rauhut, G.; Adler, T. B.; Amos, R. D.; Bernhardsson, A.; Berning, A.; Cooper, D. L.; Deegan, M. J. O.; Dobbyn, A. J.; Eckert, F.; Goll, E.; Hampel, C.; Hetzer, G.; Hrenar, T.; Knizia, G.; Köppl, C.; Liu, Y.; Lloyd, A. W.; Mata, R. A.; May, A. J.; McNicholas, S. J.; Meyer, W.; Mura, M. E.; Nicklass, A.; Palmieri, P.; Pflüger, K.; Pitzer, R.; Reiher, M.; Schumann, U.; Stoll, H.; Stone, A. J.; Tarroni, R.; Thorsteinsson, T.; Wang, M.; Wolf, A. *Molpro*, see http://www.molpro.net.

(49) Sinha, D.; Mukhopadhyay, S. K.; Chaudhuri, R.; Mukherjee, D. *Chem. Phys. Lett.* **1989**, *154*, 544−549.

(50) Stanton, J. F.; Gauss, J. *J. Chem. Phys.* **1994**, *101*, 8938−8944.

(51) Hirata, S.; Nooijen, M.; Bartlett, R. J. *Chem. Phys. Lett.* **2000**, *326*, 255−262.

(52) Knowles, P. J.; Andrews, J. S.; Amos, R. D.; Handy, N. C.; Pople, J. A. *Chem. Phys. Lett.* **1991**, *186*, 130−136.

(53) Knowles, P. J.; Hampel, C.; Werner, H.-J. *J. Chem. Phys.* **1993**, *99*, 5219−5227.

(54) Knowles, P. J.; Hampel, C.; Werner, H.-J. *J. Chem. Phys.* **2000**, *112*, 3106−3107.

(55) Jeziorski, B.; Moszynski, R.; Szalewicz, K. *Chem. Rev.* **1994**, *94*, 1887−1930.

(56) Jeziorska, M.; Bogumil, J.; Jiri, C. *Int. J. Quantum Chem.* **1987**, *32*, 149−164.

(57) Moszynski, R.; Heijmen, T. G. A.; Jeziorski, B. *Mol. Phys.* **1996**, *88*, 741−758.

(58) Zuchowski, P. S.; Podeszwa, R.; Moszynski, R.; Jeziorski, B.; Szalewicz, K. *J. Chem. Phys.* **2008**, *129*, 084101.

(59) *DALTON, A Molecular Electronic Structure Program, Release 2.0*; 2005. Available online: http://daltonprogram.org/.

(60) Lee, E. C.; Kim, D.; Jurecka, P.; Tarakeshwar, P.; Hobza, P.; Kim, K. S. *J. Phys. Chem. A* **2007**, *111*, 3446−3457.

(61) Hohenstein, E. G.; Sherrill, C. D. *J. Chem. Phys.* **2010**, *132*, 184111.

(62) Becke, A. D. *J. Chem. Phys.* **1997**, *107*, 8554−8560.

(63) Perdew, J. P.; Burke, K.; Ernzerhof, M. *Phys. Rev. Lett.* **1996**, *77*, 3865−3868.

(64) Adamo, C.; Barone, V. *J. Chem. Phys.* **1999**, *110*, 6158−6170.

(65) Zhao, Y.; Truhlar, D. G. *J. Phys. Chem. A* **2005**, *109*, 5656−5667.

(66) Grimme, S. *J. Chem. Phys.* **2006**, *124*, 034108.

(67) Schwabe, T.; Grimme, S. *Phys. Chem. Chem. Phys.* **2007**, *9*, 3397−3406.

(68) Grimme, S.; Ehrlich, S.; Goerigk, L. *J. Comput. Chem.* **2011**, *32*, 1456−1465.

(69) Perdew, J. P.; Levy, M. *Phys. Rev. B* **1997**, *56*, 16021−16028.

(70) Cohen, A. J.; Mori-Sanchez, P.; Yang, W. *J. Chem. Phys.* **2007**, *126*, 191109.

(71) Savin, A.; Flad, H.-J. *Int. J. Quantum Chem.* **1995**, *56*, 327−332.

(72) Savin, A. In *Theoretical and Computational Chemistry*; Seminario, J. M., Ed.; Elsevier: Amsterdam, 1996; Vol. *4*, pp 327−357.

(73) Iikura, H.; Tsuneda, T.; Yanai, T.; Hirao, K. *J. Chem. Phys.* **2001**, *115*, 3540−3544.

(74) Tawada, Y.; Tsuneda, T.; Yanagisawa, S.; Yanai, T.; Hirao, K. *J. Chem. Phys.* **2004**, *120*, 8425−8433.

(75) Henderson, T. M.; Janesko, B. G.; Scuseria, G. E. *J. Chem. Phys.* **2008**, *128*, 194105.

(76) Rohrdanz, M. A.; Martins, K. M.; Herbert, J. M. *J. Chem. Phys.* **2009**, *130*, 054112.

(77) Zhao, Y.; Truhlar, D. *Theor. Chem. Acc.* **2008**, *120*, 215−241.

(78) Peverati, R.; Truhlar, D. G. *J. Phys. Chem. Lett.* **2011**, *2*, 2810−2817.

(79) Vydrov, O. A.; Van Voorhis, T. *J. Chem. Phys.* **2010**, *133*, 244103.

(80) Sato, T.; Nakai, H. *J. Chem. Phys.* **2010**, *133*, 194101.

(81) Kamiya, M.; Tsuneda, T.; Hirao, K. *J. Chem. Phys.* **2002**, *117*, 6010−6015.

(82) Becke, A. D. *J. Chem. Phys.* **1996**, *104*, 1040−1046.

(83) Vydrov, O. A.; Van Voorhis, T. *J. Chem. Theory Comput.* **2012**, *8*, 1929−1934.

(84) Chai, J.-D.; Head-Gordon, M. *Phys. Chem. Chem. Phys.* **2008**, *10*, 6615−6620.

(85) Shao, Y.; Molnar, L. F.; Jung, Y.; Kussmann, J.; Ochsenfeld, C.; Brown, S. T.; Gilbert, A. T. B.; Slipchenko, L. V.; Levchenko, S. V.; O'Neill, D. P.; DiStasio, R. A., Jr; Lochan, R. C.; Wang, T.; Beran, G. J. O.; Besley, N. A.; Herbert, J. M.; Lin, C. Y.; Van Voorhis, T.; Chien, S. H.; Sodt, A.; Steele, R. P.; Rassolov, V. A.; Maslen, P. E.; Korambath, P. P.; Adamson, R. D.; Austin, B.; Baker, J.; Byrd, E. F. C.; Dachsel, H.; Doerksen, R. J.; Dreuw, A.; Dunietz, B. D.; Dutoi, A. D.; Furlani, T. R.; Gwaltney, S. R.; Heyden, A.; Hirata, S.; Hsu, C.-P.; Kedziora, G.; Khalliulin, R. Z.; Klunzinger, P.; Lee, A. M.; Lee, M. S.; Liang, W.; Lotan, I.; Nair, N.; Peters, B.; Proynov, E. I.; Pieniazek, P. A.; Rhee, Y. M.; Ritchie, J.; Rosta, E.; Sherrill, C. D.; Simmonett, A. C.; Subotnik, J. E.; Woodcock, H. L., III; Zhang, W.; Bell, A. T.; Chakraborty, A. K.; Chipman, D. M.; Keil, F. J.; Warshel, A.; Hehre, W. J.; Schaefer, H. F., III; Kong, J.; Krylov, A. I.; Gill, P. M. W.; Head-Gordon, M. *Phys. Chem. Chem. Phys.* **2006**, *8*, 3172−3191.

(86) Schmidt, M. W.; Baldridge, K. K.; Boatz, J. A.; Elbert, S. T.; Gordon, M. S.; Jensen, J. H.; Koseki, S.; Matsunaga, N.; Nguyen, K. A.; Su, S.; Windus, T. L.; Dupuis, M.; Montgomery, J. A., Jr. *J. Comput. Chem.* **1993**, *14*, 1347−1363.

(87) Weigend, F.; Ahlrichs, R. *Phys. Chem. Chem. Phys.* **2005**, *7*, 3297−3305.

(88) Murray, C. W.; Handy, N. C.; Laming, G. J. *Mol. Phys.* **1993**, *78*, 997−1014.

(89) Lebedev, V. I.; Laikov, D. N. *Doklady Mathematics* **1999**, *59*, 477−481.

(90) Gill, P. M. W.; Johnson, B. G.; Pople, J. A. *Chem. Phys. Lett.* **1993**, *209*, 506−512.

(91) Dunning, T. H., Jr. *J. Chem. Phys.* **1989**, *90*, 1007−1023.

(92) Sherrill, C. D.; Takatani, T.; Hohenstein, E. G. *J. Phys. Chem. A* **2009**, *113*, 10146−10159.

(93) Meot-Ner, M.; Hamlet, P.; Hunter, E. P.; Field, F. H. *J. Am. Chem. Soc.* **1978**, *100*, 5466−5471.

(94) Hiraoka, K.; Fujimaki, S.; Aruga, K.; Yamabe, S. *J. Chem. Phys.* **1991**, *95*, 8413−8418.

(95) Miyoshi, E.; Yamamoto, N.; Sekiya, M.; Tanaka, K. *Mol. Phys.* **2003**, *101*, 227−232.

(96) Pieniazek, P. A.; Krylov, A. I.; Bradforth, S. E. *J. Chem. Phys.* **2007**, *127*, 044317.

(97) Rapacioli, M.; Spiegelman, F.; Scemama, A.; Mirtschink, A. *J. Chem. Theory Comput.* **2011**, *7*, 44−55.

(98) Diri, K.; Krylov, A. I. *J. Phys. Chem. A* **2012**, *116*, 653−662.

(99) Mo, Y.; Song, L.; Lin, Y.; Liu, M.; Cao, Z.; Wu, W. *J. Chem. Theory Comput.* **2012**, *8*, 800−805.

(100) Hobza, P.; Sponer, J. *J. Am. Chem. Soc.* **2002**, *124*, 11802−11808.

(101) Jurecka, P.; Sponer, J.; Hobza, P. *J. Phys. Chem. B* **2004**, *108*, 5466−5471.

(102) Comparing the two LRD variants tested (with and without nonlocal contributions to the C6 coefficients), suggests that Orel26rad benefits from these nonlocal contributions, which lower the MAD by

0.3 kcal $mol^{-1}$. Similarly, LC-VV10, which is fully nonlocal, slightly outperforms the best LC-dDsC variant (LC-$\omega$PBEB95-dDsC), in which no explicitly nonlocal terms are considered.

(103) For the equilibrium geometry of the neutral antiparallel thiophene dimer (T2_AP) with interaction energies of −1.55 and −1.53 kcal $mol^{-1}$ excellent agreement between HF+Disp and MP2/6-31G*(0.25) is obtained.